

Cite this: *Soft Matter*, 2011, **7**, 9410

www.rsc.org/softmatter

PAPER

Flower micelles of poly(*N*-isopropylacrylamide) with azobenzene moieties regularly inserted into the main chain†

Olivier Boissiere,^a Dehui Han,^a Luc Tremblay^b and Yue Zhao^{*a}

Received 18th June 2011, Accepted 1st August 2011

DOI: 10.1039/c1sm06149f

Hydrophobically modified poly(*N*-isopropylacrylamide) (PNIPAM) with an azobenzene-containing short segment repeatedly inserted into the main chain was synthesized. The reversible *trans*–*cis* photoisomerization of azobenzene was found to exert little effect on the lower critical solution temperature (LCST) or the cloud point of PNIPAM in aqueous solution. The characterization results of variable-temperature ¹H NMR, TEM and DLS indicate the formation of flower micelles in cold water with hydrated PNIPAM. The segregation of azobenzene moieties in the micelle core from PNIPAM chains in micelle corona may explain the absence of an effect of photoisomerization of the chromophore on the LCST of PNIPAM. While the micelle core could react during the photoisomerization by swelling (with azobenzene in the *cis* form) or contracting (in the *trans* form) due to a polarity change, PNIPAM undergoes the hydration–dehydration transition according to its LCST. Another interesting finding is that the flower micelles resulting from this type of hydrophobically modified PNIPAM exhibit a much reduced propensity for inter-micellar association and could remain well dispersed at $T > \text{LCST}$ of PNIPAM, in sharp contrast with flower micelles formed by α,ω -telechelic PNIPAM. The multiple intrachain folding arising from this new PNIPAM structure appears to be the origin of the enhanced dispersion stability. With azobenzene groups stacked together forming the micelle core, the multiple loops for individual PNIPAM chains could reduce the number of inter-micellar bridge chains and restrict the chain entanglements upon dehydration of PNIPAM, which, consequently, reduce the propensity for micellar aggregation.

Introduction

There is much interest in thermosensitive water-soluble polymers exhibiting a lower critical solution temperature (LCST) due to their potential for applications.¹ Among the most studied polymers are poly(*N*-isopropylacrylamide) (PNIPAM),² poly[oligo (ethylene glycol) methacrylate] (POEGMA)³ and poly(*N,N*-dimethylaminoethyl methacrylate) (PDMAEMA).⁴ The LCST, below which the polymer is soluble (hydrated) and above which the polymer becomes insoluble (dehydrated), obviously is an important property for applications, and the ability to control it is desired. There are various means to change the LCST of a given polymer. For instance, incorporating either hydrophilic or hydrophobic comonomer units could increase or decrease, respectively, the LCST.⁵ One can also modify it by exploiting some polymer chain topological effects.⁶ However, it is

particularly appealing if the LCST can be reversibly varied between two temperatures by exposure to light at two different wavelengths, which means a switchable polymer water solubility at a constant temperature. To achieve this, the basic method consists in making the polymer contain a number of photochromic moieties that can undergo a reversible photochemical reaction such as the *trans*–*cis* photoisomerization of azobenzene. In most cases, azobenzene has been incorporated into the polymer structure as side groups; in case the *trans*–*cis* photoisomerization induces a change in the polarity of the chromophore, a shift of the LCST to either higher or lower temperatures could be observed, but the photoinduced (and reproducible) switching effect generally is very small (a few degrees).⁷ More recently, hydrophobically modified telechelic polymers with azobenzene moieties as chain end groups were prepared and investigated.^{8,9} The *trans*–*cis* photoisomerization was also found to induce a very small change of the LCST, though there is a reported over 10 °C increase of LCST with a low-molecular-weight PNIPAM.¹⁰

In the present study, we prepared a different version of photosensitive, hydrophobically modified PNIPAM by inserting azobenzene moieties regularly onto the main chain, and investigated the effect of the reversible *trans*–*cis* photoisomerization on

^aDépartement de chimie, Université de Sherbrooke, Sherbrooke, Québec, Canada J1K 2R1. E-mail: yue.zhao@usherbrooke.ca

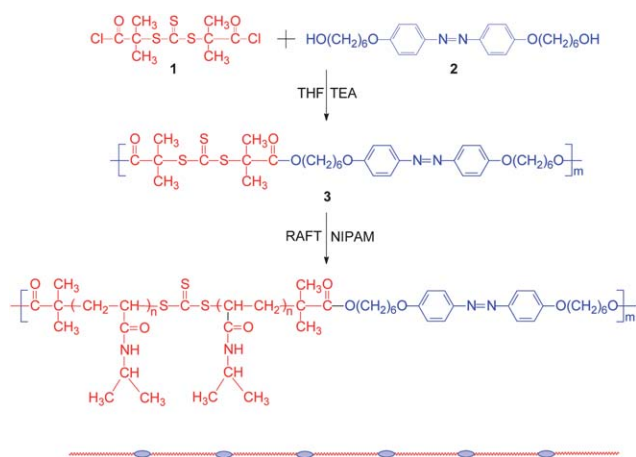
^bDépartement de médecine nucléaire et de radiobiologie and Centre d'imagerie moléculaire de Sherbrooke, Université de Sherbrooke, Sherbrooke, Québec, Canada J1H 5N4

† Electronic supplementary information (ESI) available. See DOI: 10.1039/c1sm06149f

the LCST of PNIPAM. As will be shown below, little effect was observed with this new structure. However, the characterization results revealed that similar to telechelic PNIPAM,^{9,11,12} the polymer could form flower micelles in cold water with hydrated PNIPAM chains. While the micelle core formed by azobenzene moieties could respond to the *trans*–*cis* photoisomerization by swelling or contracting, the spatially segregated hydrophobic domain would have limited influence on the PNIPAM micelle corona that could undergo the hydration–dehydration transition basically at the same temperature with azobenzene in either the *trans* or the *cis* form. This result suggests that aggregation of photochromic moieties from hydrated PNIPAM chains might be the reason why the photoisomerization has limited effect on the LCST of the polymer. Another interesting finding of this study is that the flower micelle formed by this type of hydrophobically modified PNIPAM exhibits a much reduced propensity for intermicellar association or aggregation upon dehydration of PNIPAM, as compared to telechelic PNIPAM. The dispersion of micelles could remain stable at $T > \text{LCST}$. This phenomenon may be explained by the multiple chain folding arising from this new structure.

Results and discussion

Details on the polymer synthesis and the characterization techniques used are given in the ESI†. To our knowledge, this is the first PNIPAM with azobenzene moieties regularly inserted into the main chain. For this reason, the essence of the synthesis and characterization is summarized below. Scheme 1 shows the synthetic procedure used to obtain this new structure of hydrophobically modified PNIPAM, referred to as multi-azo-PNIPAM, *via* reversible addition fragmentation chain transfer polymerization (RAFT). The key step is the use of step-growth polymerization to obtain an azobenzene-containing multifunctional chain transfer agent (CTA) which is then utilized to grow PNIPAM. Using a polytrithiocarbonate RAFT agent with $M_n \approx 4600 \text{ g mol}^{-1}$, two samples of multi-azo-PNIPAM with $M_n \approx 22\,000$ and $37\,000 \text{ g mol}^{-1}$, denoted as P1 and P2 hereafter, were obtained by varying the feeding ratio of NIPAM to



Scheme 1 Synthetic route to and schematic illustration of hydrophobically modified PNIPAM with azobenzene units regularly inserted in the main chain.

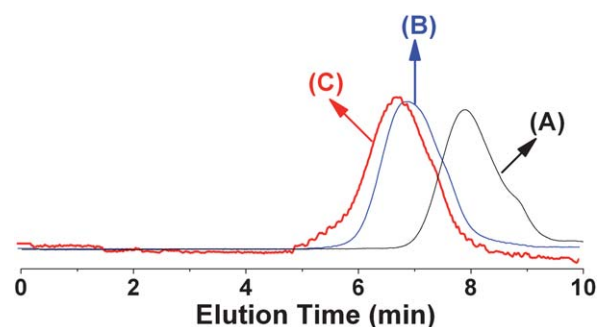


Fig. 1 SEC traces of (a) azobenzene-containing polytrithiocarbonate RAFT agent ($M_n = 4600$, PDI = 1.60), (b) multi-azo-PNIPAM sample P1 ($M_n = 22\,000$, PDI = 1.70) and (c) P2 ($M_n = 37\,000$, PDI = 1.80) prepared by using the polytrithiocarbonate RAFT agent.

the RAFT agent. Fig. 1 shows their SEC curves. Despite the use of RAFT, the two samples have a relatively large PDI (1.7–1.8), originating from the large PDI of the azobenzene CTA synthesized by a step-growth polymerization. The amounts of PNIPAM with respect to azobenzene moieties in the two samples were determined from their ^1H NMR spectra (Fig. S1 in ESI†). Using the M_n (SEC) of the CTA, the NMR analysis resulted in $M_n \approx 31\,600$ and $44\,300 \text{ g mol}^{-1}$ for P1 and P2, respectively, which are higher than the SEC results using PS standards. The two samples contain the same number of azobenzene units on the main chain (~ 7) but differ in the PNIPAM chain length between two hydrophobic segments (~ 40 NIPAM units for P1 and 56 for P2 from NMR analysis). We mention that the average number of azobenzene units calculated from the SEC-based M_n may contain appreciable uncertainty. Nevertheless, the described synthesis method ensures the insertion of multiple azobenzene moieties into the main chain and the same average PNIPAM chain length separated by two hydrophobic segments. It should be emphasized that this feature is what makes this type of hydrophobically modified PNIPAM different from α,ω -telechelic polymers.

The effect of the *trans*–*cis* photoisomerization of azobenzene on the LCST was investigated with the two samples P1 and P2 by measuring the cloud point of their aqueous solution. Fig. 2 shows the results obtained at the polymer concentration of 10 mg mL^{-1} , with azobenzene in both the *trans* (before UV exposure) and the *cis* form (after UV). In the latter case, the polymer solution at 10°C was exposed to UV light to reach the photostationary state rich in the *cis* isomer before being subjected to stepwise heating and measurement of the solution transmittance. Under the used conditions, most *cis* isomers of azobenzene remained at the end of measurement with the solution heated to 50°C , due to a very slow thermal relaxation of the azobenzene moiety (Fig. S2†). It can be seen from the results that, on the one hand, with *trans* azobenzene, *i.e.*, before UV exposure, the cloud point of P1 can hardly be noticed, as the transmittance decreases very slightly at $\sim 31^\circ\text{C}$, around the LCST of PNIPAM. As for P2, the decrease in transmittance becomes more important, but is still limited. This result suggests the absence or very limited extent of polymer chain aggregation for P1 and P2 upon dehydration of PNIPAM chains. Their stable water solubility can also be appreciated from the photographs in the inset showing transparent P1 and translucent P2 solution at 50°C , well above the LCST of PNIPAM.

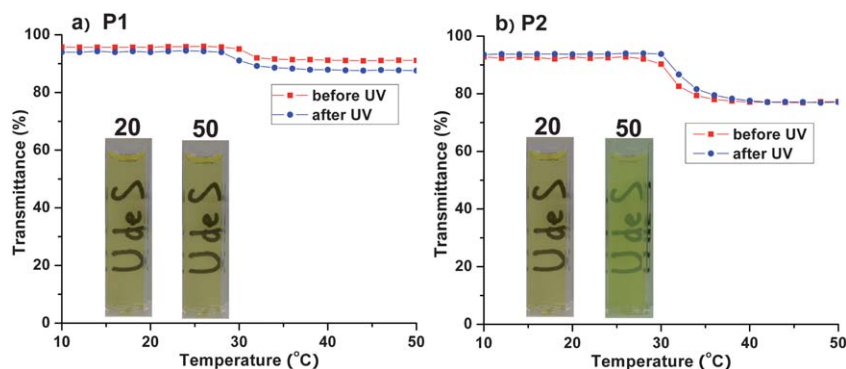


Fig. 2 Change in transmittance (measured at 700 nm) of aqueous solutions of (a) P1 and (b) P2 at a polymer concentration of 10 mg mL⁻¹ before and after UV exposure. In the inset, the photographs taken at two temperatures show the visually observable transmittance change.

On the other hand, as can be seen for both samples, the photo-induced *trans*-*cis* isomerization of azobenzene exerts little effect on the apparent cloud point temperature. The slight differences are likely to fall within experimental uncertainty of these measurements. The absence of a significant effect of the photoisomerization of azobenzene on the cloud point of PNIPAM is reminiscent of the observations reported with the telechelic polymers with azobenzene moieties at the chain ends.^{8,9} This result indicates that by placing more chromophore units in the main chain could not enhance the photoswitching of the LCST of PNIPAM. More surprising is the observed very small transmittance decrease of the multi-azo-PNIPAM, which is in sharp contrast with the behaviors of PNIPAM or telechelic PNIPAM, for which a solution at the used polymer concentration and temperatures well above the LCST is known to turn completely opaque due to a large decrease of the solution transmittance as a result of the formation of large mesoglobules.^{9,11,12}

How does one explain the above results? Variable-temperature ¹H NMR measurements provide us with some insight into what happens in the solution. Fig. 3 shows the ¹H NMR spectra of P1 in D₂O (5 mg mL⁻¹), with either *trans* azobenzene (a) or *cis*

azobenzene (b), recorded at various temperatures upon stepwise heating from 10 °C, the resonance signals in the 6–8 ppm region for aromatic protons being amplified by a factor of 10 for the sake of clarity (only spectra at the chosen temperatures are shown although a spectrum was recorded for every increase of 2 °C). On one hand, at 10 °C all peaks of PNIPAM can clearly be seen, at ~0.9 and 3.6 ppm for two CH₃ and one CH of the isopropyl group, respectively, and at 1.2 and 1.5 ppm for CH₂ and CH of the main chain (overlapped with signals from CH₂ of the hydrophobic segments). Upon heating of the solution to around the LCST of PNIPAM, these peaks become less intense as a result of reduced hydration of PNIPAM chains (reduced chain mobility). On the other hand, the resonance signals of *trans* azobenzene could not be detected even at 10 °C, indicating that these hydrophobic moieties are not solvated even though the PNIPAM chains interconnected by them are. By contrast, after exposure of the solution to UV light at 10 °C, the signals of *cis* azobenzene become visible, indicating that the *cis* isomer has an increased polarity¹³ and could be partially hydrated in cold water. Upon heating, as PNIPAM chains undergo the hydration–dehydration transition related to the LCST, signals of *cis*

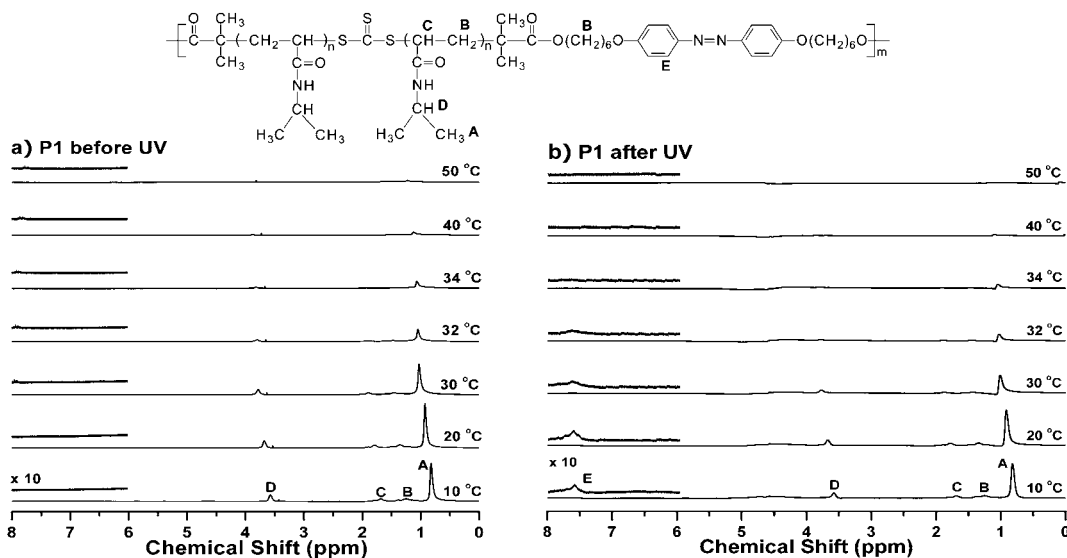


Fig. 3 Variable-temperature ¹H NMR spectra of P1 in D₂O (5 mg mL⁻¹) recorded before (a) and after UV exposure (b).

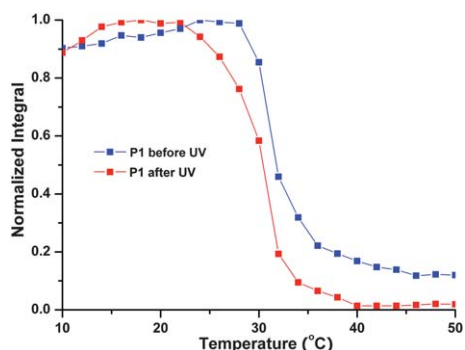


Fig. 4 Normalized integral of the resonance peak at ~ 0.9 ppm of PNIPAM vs. temperature upon heating of the P1 solution (5 mg mL^{-1}) before and after UV exposure (Fig. 3).

azobenzene also become invisible, indicating the dehydration of the whole polymer including azobenzene segments. Fig. 4 shows the plot of the integral of the resonance peak at 0.9 ppm, which is the most prominent, as a function of temperature for the polymer solution both before and after UV irradiation. The dehydration of PNIPAM chains clearly occurs at ~ 32 °C, and the conversion of *trans* azobenzene to the *cis* isomer results in no meaningful effect on the LCST of PNIPAM within the experimental error. Similar observations were obtained with P2.

Therefore, the NMR results are consistent with the transmittance measurements (Fig. 2) and confirm that the photoisomerization has negligible effect on the LCST of PNIPAM. But more importantly, the NMR results suggest an explanation for this. In cold water at $T < \text{LCST}$, PNIPAM chains are soluble, but hydrophobic azobenzene moieties on the main chain already exist in an aggregated state, meaning the formation of flower micelles. While the *trans*–*cis* photoisomerization can well occur inside the micelle core and induce a polarity change, it would affect little PNIPAM chains since azobenzene moieties are spatially segregated from them. This explanation may apply to the telechelic PNIPAM with azobenzene end groups as well.⁹ Regarding the much enhanced dispersion stability at $T > \text{LCST}$, a possible explanation resides in the fact that as compared to the flower micelle formed by telechelic PNIPAM, the flower micelle of multi-azo-PNIPAM means that each PNIPAM chain can undergo multiple folding giving rise to multiple loops. At $T > \text{LCST}$, PNIPAM chains undergo the hydration–dehydration transition, but the flower micelles remain well dispersed in water.

The multiple chain loops may prevent the association of micelles and the formation of large mesoglobules, which accounts for the small solution transmittance decrease.

The formation of flower micelles of multi-azo-PNIPAM was confirmed by DLS analysis and TEM observations. The reversible size change of the micelles in response to temperature switching between below and above the LCST of PNIPAM and to UV and visible light exposure inducing the isomerization of azobenzene was also observed from these measurements. An example of the representative DLS results is given in Fig. 5 showing the distribution of volume-weighted hydrodynamic diameters (D_H) for the aqueous solutions of P1 and P2 at 20 °C (below LCST) and 50 °C (above LCST). First, at 20 °C before UV exposure (*trans* azobenzene), both samples form small micelles with P2 having a larger average D_H (~ 21 nm) than P1 (~ 17 nm) likely due to their difference in the PNIPAM chain length. Upon heating to 50 °C, the average sizes of their micelles increase and the size distributions become larger. This should be caused by some inter-micellar association due to the dehydration of PNIPAM chains. The aggregation for P2 (D_H increases to 33 nm) is more important than P1 (D_H to 25 nm), which is in agreement with the solution transmittance change (Fig. 2). Secondly, keeping the solution temperature at 20 °C, after exposure to UV light, which converts *trans* azobenzene to the *cis* isomer, the micelles of both P1 and P2 also display an increase in their average sizes (D_H increase to ~ 22 and 27 nm for P1 and P2 respectively). This result implies that the micelle core could be hydrated to some extent with *cis* azobenzene groups, which also corroborates well with the ^1H NMR measurements (Fig. 3). In other words, with the more polar *cis* isomer, the micelle core could be “opened” slightly allowing water to flow in and interact with the azobenzene groups. Even though the photoinduced salvation of the micelle core may be limited, the swelling results in an observable size increase. The micelles could also be observed on TEM. As an example, Fig. 6 shows images of micelles of P1 with its aqueous solution cast at 20 °C before and after UV irradiation, and at 70 °C without UV irradiation. Since the images were recorded after drying, comparison of the micelle size with *trans* and *cis* azobenzene is not straightforward. However, the absence of significant micelle aggregation at temperatures well above the LCST of PNIPAM is visible.

Fig. 7 shows a schematic recapitulation of the flower micelles of multi-azo-PNIPAM. As compared to the flower micelles formed by α,ω -telechelic PNIPAM, the most interesting feature

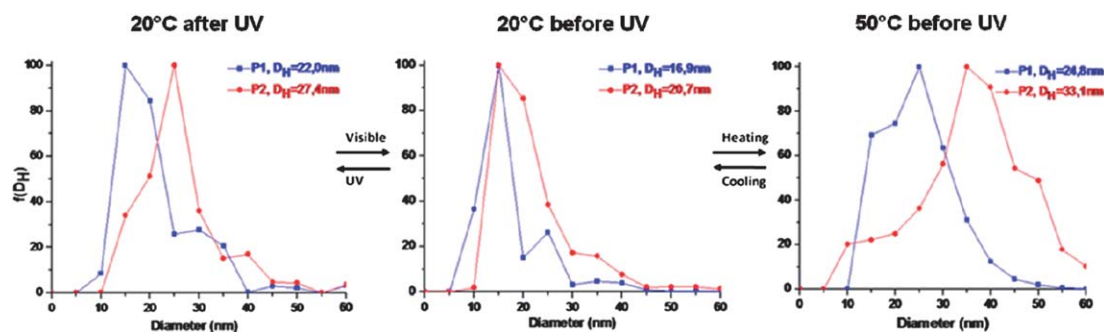


Fig. 5 Distribution of volume-weighted hydrodynamic diameters of P1 and P2 in water (10 mg mL^{-1}) in response to temperature change (between 20 and 50 °C) and in response to UV (*trans*–*cis* isomerization) and visible light exposures (*cis*–*trans* isomerization).

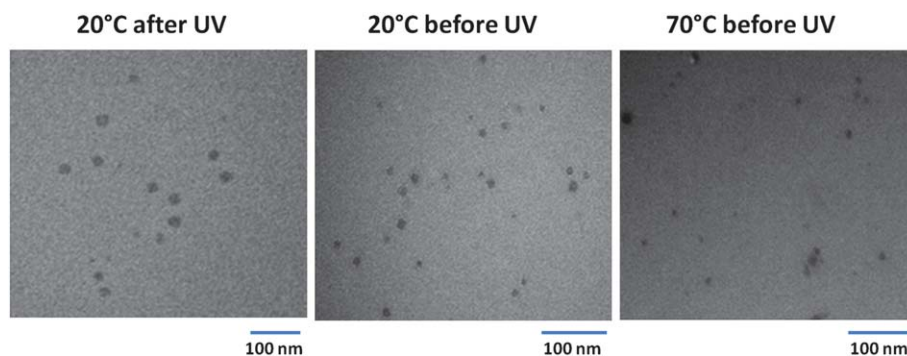


Fig. 6 TEM images of flower micelles of P1 cast from solutions at 20 °C before and after UV exposure and at 70 °C without UV exposure.

of this new type of flower micelles is the remarkably reduced propensity for association at temperatures both below and above the LCST of PNIPAM. In cold water at 10 °C, no gel formation was observed even at a polymer concentration of 40 mg mL⁻¹, while for telechelic hydrophobically modified PNIPAM, a sol-gel transition could be observed at such high polymer concentrations as a result of the formation of a network of micelles connected by bridging telechelic chains.¹² At $T > \text{LCST}$, even with a dilute concentration of telechelic polymers, the solution transmittance drops considerably at the cloud point as a result of the association of micelles upon the dehydration of PNIPAM chains. As a matter of fact, the solution transmittance of a telechelic PNIPAM with two azobenzene end groups was down to near 100% at 1 mg mL⁻¹ and dropped by ~50% at 0.2 mg mL⁻¹.⁹ This contrasts sharply with the small transmittance decrease for the solutions of P1 and P2 at a much higher polymer concentration of 10 mg mL⁻¹ (Fig. 2). At the cloud point temperature, the transmittance of the P1 solution decreased by nearly 5% and that of P2 by about 16% only. As mentioned above, the multiple folding arising from the presence of regularly separated azobenzene moieties in the main chain would account for the differences. On one hand, upon dehydration of telechelic PNIPAM chains at $T > \text{LCST}$, the aggregation of flower micelles is favored by the bridge chains whose hydrophobic chain ends can be in different micelles^{9,11,12} or by the presence of free chains that can entangle with the single loop formed by each folding PNIPAM chain. In the case of multi-azo-PNIPAM, the presence of several azobenzene units in the main chain means that their aggregation to form the micelle core induces multiple folding from a single chain, resulting in more but smaller chain loops than telechelic PNIPAM. This is similar to the many small loops formed when a hydrophobically modified poly(acrylic acid) (PAA) containing a number of azobenzene side groups is associated with micelles of a neutral surfactant.¹⁴ It is easy to imagine that such multi-folded chains can hardly participate in the

formation of different micelles and act as bridge chains. In other words, the intra-molecular multi-folding could reduce considerably the number of bridge chains in the solution of flower micelles. On the other hand, smaller loops should also make their mutual interactions or entanglements much more difficult to develop. This topology effect is in line with a number of recent reports showing that the chain topology by forming cycles or loops can affect the polymer's solubility or dispersion stability in water.⁶ Multi-azo-PNIPAM can also be regarded as a multiblock (AB)_n where A is PNIPAM and B is the very short azobenzene hydrophobic segment. It is interesting to compare it with a multiblock copolymer (AB)_n where A and B are both long-chain polymers. In the latter case, in a block-selective solvent (say, bad for B), each B block collapses into a globule separated by two soluble A blocks, and there is no multiple chain folding due to the absence of association of insoluble B blocks.^{15,16}

Conclusions

We synthesized a new type of hydrophobically modified PNIPAM with multiple azobenzene-containing short hydrophobic segments regularly inserted into the main chain. This structure differs from telechelic PNIPAM having only two hydrophobic segments at the chain ends. The characterization results clearly show that such multi-azo-PNIPAM self-assembles into flower micelles at temperatures below the LCST of PNIPAM due to aggregation of the hydrophobic azobenzene moieties. The spatial segregation of the chromophore from hydrated PNIPAM chains is likely to be the reason why its *trans-cis* photoisomerization displays negligible effect on the LCST of PNIPAM. Interestingly, the flower micelles arising from this new chain structure exhibit a much reduced propensity for inter-micellar association upon dehydration of PNIPAM; they could remain well dispersed at temperatures well above the LCST, which is in sharp contrast with the lower micelles formed by telechelic PNIPAM. This stability in water may originate from the multiple chain-folding of multi-azo-PNIPAM chains as a result of aggregation of azobenzene moieties. As compared to one loop formed by each chain of telechelic PNIPAM, the multiple and smaller loops of each multi-azo-PNIPAM chain would reduce the number of bridge chains and prevent chain entanglements that favor the inter-micellar association. This topology effect stabilizing the micellar dispersion is of fundamental interest and can be explored in other systems.

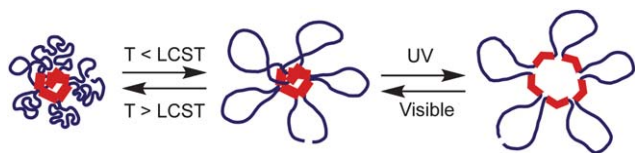


Fig. 7 Schematic illustration of the photo- and thermoresponsive behaviors of the flower micelle formed through multiple folding of individual chains.

Acknowledgements

We acknowledge the financial support from the Natural Sciences and Engineering Research Council of Canada (NSERC) and le Fonds québécois de la recherche sur la nature et les technologies of Québec (FQRNT). YZ is a member of the FQRNT-funded Center for Self-Assembled Chemical Structures.

Notes and references

- (a) Y. Qiu and K. Park, *Adv. Drug Delivery Rev.*, 2001, **53**, 321; (b) E. S. Gil and S. M. Hudson, *Prog. Polym. Sci.*, 2004, **29**, 1173; (c) L. E. Bromberg and E. S. Ron, *Adv. Drug Delivery Rev.*, 1998, **31**, 197; (d) I. Luzinov, S. Minko and V. Tsukruk, *Prog. Polym. Sci.*, 2004, **29**, 635.
- (a) H. G. Schild, *Prog. Polym. Sci.*, 1992, **17**, 163; (b) X. Yin, P. S. Stayton and A. S. Hoffman, *Biomacromolecules*, 2006, **7**, 1381; (c) A. J. Convertine, N. Ayres, C. W. Scales, A. B. Lowe and C. L. McCormick, *Biomacromolecules*, 2004, **5**, 1177.
- (a) J. F. Lutz, O. Akdemir and A. Hoth, *J. Am. Chem. Soc.*, 2006, **128**, 13046; (b) J. H. Ryu, R. T. Chacko, S. Jiwanich, S. Bickerton, R. P. Babu and S. J. Thayumanavan, *J. Am. Chem. Soc.*, 2010, **132**, 17227; (c) F. D. Jochum, P. J. Roth, D. Kessler and P. Theato, *Biomacromolecules*, 2010, **11**, 2432.
- (a) F. M. Li, S. J. Chen, F. S. Du, Z. Q. Wu and Z. C. Li, *ACS Symp. Ser.*, 1999, **726**, 266; (b) X. Z. Jiang, Z. S. Ge, J. Xu, H. Liu and S. Y. Liu, *Biomacromolecules*, 2007, **8**, 3184; (c) A. S. Lee, V. Bütün, M. Vamvakaki, S. P. Armes, J. A. Pople and A. P. Gast, *Macromolecules*, 2002, **35**, 8540.
- (a) L. C. Leroux, E. Roux, D. Le Garrec, K. L. Hong and D. C. Drummond, *J. Controlled Release*, 2001, **72**, 71; (b) H. Feil, Y. H. Bae, J. Feijen and S. W. Kim, *Macromolecules*, 1993, **26**, 2496; (c) R. Yoshida, K. Sakai, T. Okano and Y. Sakurai, *J. Biomater. Sci., Polym. Ed.*, 1994, **6**, 585.
- (a) X. P. Qiu, F. Tanaka and F. M. Winnik, *Macromolecules*, 2007, **40**, 7069; (b) S. Honda, T. Yamamoto and Y. Tezuka, *J. Am. Chem. Soc.*, 2010, **132**, 10251; (c) A. Saha and S. Ramakrishnan, *Macromolecules*, 2008, **41**, 5658; (d) Y. Zhao, L. Tremblay and Y. Zhao, *Macromolecules*, 2011, **44**, 4007.
- (a) M. Irie, *Adv. Polym. Sci.*, 1993, **110**, 49–65; (b) A. Desponds and R. Freitag, *Langmuir*, 2003, **19**, 6261; (c) K. Sumaru, M. Kameda, T. Kanamori and T. Shinbo, *Macromolecules*, 2004, **37**, 4949–4955; (d) T. Shimoboj, L. Ding and A. S. Hoffman, *Bioconjugate Chem.*, 2002, **13**, 915; (e) Y. Zhao, L. Tremblay and Y. Zhao, *J. Polym. Sci., Part A: Polym. Chem.*, 2010, **48**, 4055.
- F. D. Jochum, L. Z. Borg, L. Roth and P. Theato, *Macromolecules*, 2009, **42**, 7854.
- N. Ishii, R. Obeid, X.-P. Qiu, J.-I. Mamiya, T. Ikeda and F. M. Winnik, *Mol. Cryst. Liq. Cryst.*, 2010, **529**, 60.
- H. Akiyama and N. Tamaoki, *Macromolecules*, 2007, **40**, 5129.
- P. Kujawa, H. Watanabe, F. Tanaka and F. M. Winnik, *Eur. Phys. J. E*, 2005, **17**, 129.
- T. Koga, F. Tanaka, R. Motokawa, S. Koizumi and F. M. Winnik, *Macromolecules*, 2008, **41**, 9413.
- (a) X. Tong, G. Wang, A. Soldera and Y. Zhao, *J. Phys. Chem. B*, 2005, **109**, 20281; (b) Y. Zhao, *J. Mater. Chem.*, 2009, **19**, 4887; (c) J.-M. Schumers, C.-A. Fustin and J.-F. Gohy, *Macromol. Rapid Commun.*, 2010, **31**, 1588; (d) B. Y. Wang, H. Xu and X. Zhang, *Adv. Mater.*, 2009, **21**, 2849.
- J. Ruchmann, S. C. Sebai and C. Tribet, *Macromolecules*, 2011, **44**, 604.
- L. Hong, F. Zhu, J. Li, T. Ngai, Z. Xie and C. Wu, *Macromolecules*, 2008, **41**, 2219.
- Q. Zhang, J. Ye, Y. Lu., T. Nie, D. Xie, Q. Song, H. Chen, G. Zhang, Y. Tang, C. Wu and Z. Xie, *Macromolecules*, 2008, **41**, 2228.

Thermo- and Photosensitive Flower Micelle of Poly(*N*-isopropylacrylamide) with Azobenzene Moieties Regularly Inserted in the Main Chain

Olivier Boissiere,¹ Dehui Han,¹ Luc Tremblay,² Yue Zhao^{1,*}

1. Polymer Synthesis

Materials. All chemicals were purchased from Aldrich unless otherwise stated. Prior to use, tetrahydrofuran (THF, 99%) was refluxed with sodium and a small amount of benzophenone and distilled; dichloromethane (DCM, 99%) was refluxed with CaH₂ and distilled; triethylamine (TEA) (≥99%) was refluxed with *p*-toluenesulfonyl chloride (Fluka, ≥99%) and distilled. Potassium carbonate (K₂CO₃, 99%), potassium iodide (KI, 99%), 6-chlorohexanol (96%), 4-nitrophenol (≥99%), oxalyl chloride (2.0 M in methylene chloride) and ethanol (95%) were used without purification. Azobisisobutyronitrile (AIBN, 98%) was recrystallized from methanol and *N*-isopropylacrylamide (NIPAM, 97%) was recrystallized from hexane. 4,4'-Dihydroxyazobenzene and *S,S'*-bis(α,α' -dimethyl- α'' -acetic acid)-trithiocarbonate were synthesized according to reported methods.^{10,11}

Synthesis of 4,4'-Dihydroxyhexyloxyazobenzene (2 in Scheme 1). 4,4'-Dihydroxyazobenzene (23.4 mmol, 5.0 g), 6-chlorohexanol (56.2 mmol, 7.7 g), K₂CO₃ (56.2 mmol, 7.8 g), ethanol (250 mL) and trace of KI were added into a 500 mL one-necked flask. The mixture was refluxed at 85 °C for 36 h under stirring. After evaporating ethanol, the residue was poured into water (1 L, pH=12). The yellow precipitate was washed with copious water and further recrystallized from methanol to give a yellow crystal (6.6 g with 68% yield). ¹H-NMR (300 MHz, δ ppm, DMSO-*d*₆): 7.82 (d, 4H, *o*-ArH to -N=N-), 7.11 (d, 4H, *o*-ArH to OCH₂(CH₂)₄CH₂OH), 4.40 (t, 2H, OCH₂(CH₂)₄CH₂OH), 4.09 (t, 4H, OCH₂(CH₂)₄CH₂OH), 3.75 (m, 4H, OCH₂(CH₂)₄CH₂OH), 1.30-1.86 (m, 16H, OCH₂(CH₂)₄CH₂OH).

Synthesis of Azobenzene-Containing Multifunctional Chain Transfer Agent (3). The polytrithiocarbonate RAFT agent was prepared by step-growth polymerization of **1** with **2** (Scheme 1). A typical preparation process is as follows. In the presence of argon, oxalyl chloride (9.0 mL, 18 mmol) was added dropwise to *S,S'*-bis(α,α' -dimethyl- α'' -acetic acid)-trithiocarbonate (BDATC) (0.54 g, 1.94 mmol). At the end of addition, the reaction mixture was heated to 60 °C for 3 h, resulting in the formation of a bright yellow solution. The excess oxalyl chloride was removed completely under reduced pressure to obtain a yellow solid (**1** in Scheme 1). Afterward, a THF solution of **1** (1.94 mmol) was added dropwise to 10.0 mL of THF solution of **2** (0.75 g, 1.8 mmol) containing 0.6 mL of TEA as catalyst. After the reaction mixture was stirred for 36 h at room temperature, the THF solution was concentrated and then precipitated into hexane to obtain the polytrithiocarbonate RAFT agent as a dark yellow solid (1.06 g with 85% yield). ¹H-NMR (300 MHz, δ ppm, CDCl₃): 7.80 (q, 4H, *o*-ArH to -N=N-), 6.97 (q, 4H, *o*-ArH to -OCH₂(CH₂)₄CH₂O-), 4.0-4.3 (m, 8H, -OCH₂(CH₂)₄CH₂O-), 1.98 (m, 12H, -C(CH₃)₂S(C=S)S C(CH₃)₂-), 1.40-1.80 (m, 16H, -OCH₂(CH₂)₄CH₂O-). M_n=4600, PDI=1.60, according to size exclusion chromatography (SEC) measurements using polystyrene (PS) standards. The estimated average number of trithiocarbonate groups (and thus the number of azobenzene moieties) in the macro-CTA is about 7. Also, in order to have azobenzene moieties in the main chain while growing PNIPAM chains using RAFT, an excess of **1** was used for the condensation reaction with **2**, which, statistically, should make the macro-CTA bear two trithiocarbonate end groups.

Synthesis of PNIPAM with Regularly Inserted Azobenzene Moieties in the Main Chain. A typical RAFT polymerization of NIPAM using the polytrithiocarbonate RAFT agent is as follows. **3** (82.8 mg, 0.018 mmol), AIBN (0.3 mg, 0.0018 mmol), NIPAM (1.5 g, 0.013 mol) and 4.0 mL THF were added into a 10-mL flask with a stirring bar. The solution was deoxygenated by bubbling argon for 30 min and then placed into an oil bath preheated to 70 °C. The polymerization was allowed to proceed for 2 h with the mixture under stirring. The polymer was collected after two precipitations of a THF solution in diethyl ether. This reaction gave rise to a sample of multi-azo-PNIPAM with M_n (NMR) \sim 31600 g/mol (using SEC-based M_n of **3**). $^1\text{H-NMR}$ (300 MHz, δ ppm, CDCl_3): 7.80 (broad, 4H, *o*-ArH to $-\text{N}=\text{N}-$), 6.97 (broad, 4H, *o*-ArH to $-\text{OCH}_2(\text{CH}_2)_4\text{CH}_2\text{O}-$), 6.90-5.70 (broad, 1H, NH in PNIPAM), 4.30-3.90 (broad, 9H, $-\text{C}(\text{CH}_3)_2\text{S}(\text{C}=\text{S})\text{SC}(\text{CH}_3)_2\text{COOCH}_2(\text{CH}_2)_4\text{CH}_2\text{O}-$ and CH_3CHCH_3 in PNIPAM), 2.30-1.20 (broad, 31H, $-\text{C}(\text{CH}_3)_2\text{S}(\text{C}=\text{S})\text{SC}(\text{CH}_3)_2\text{COOCH}_2(\text{CH}_2)_4\text{CH}_2\text{O}-$ and aliphatic main chain), 1.13 (s, 6H, CH_3CHCH_3 in PNIPAM).

2. Characterisations

Unless otherwise stated, all polymer solutions were prepared in deionised water at the concentration of 10 mg/mL; in cold water at 10 °C, all samples of multi-azo-PNIPAM were well dissolved. The cloud point measurements were conducted by taking UV-vis spectra with a spectrophotometer (Varian 50 Bio) while heating the solution (4 mL) in a cuvette held in a thermostat sample holder (Varian SPVF). The change in solution transmittance at 700 nm, which is far from absorption of azobenzene, was recorded as a function of temperature. The solution was heated stepwise with an interval of 2 °C and held at each temperature for 5 min for thermal equilibrium before the spectral taking. For the measurements with azobenzene in the *cis* form, the polymer solution was exposed to UV light at 10 °C for the *trans-cis* isomerization, the UV beam being generated from a spot-curing system (Novacure) with a UV filter (354 nm, \sim 50 mW/cm²). After the photostationary state rich in *cis* azobenzene was obtained, the cloud point measurements were carried out. The same spot-curing system was also used to produce visible light with a visible filter (440 nm, \sim 5 mW/cm²) for the reverse *cis-trans* isomerization of azobenzene.

While a Bruker 300 MHz spectrometer (AC 300) was used to record ^1H NMR spectra for general sample characterizations, variable-temperature ^1H NMR spectra of multi-azo-PNIPAM dissolved in D_2O were recorded on a Varian 600 MHz spectrometer (INOVA system). For these measurements, the polymer concentration was 5 mg/mL. Other experimental conditions were the same as in the cloud point measurements, i. e. solution temperature raised stepwise by 2 °C with the solution held at a given temperature for 5 min before taking the spectrum. Dynamic light scattering (DLS) measurements were carried out on a Brookhaven goniometer (BI-200) equipped with a highly sensitive avalanche photodiode detector (Brookhaven, BI-APD), a digital correlator (Brookhaven, TurboCorr) that calculates the photon intensity autocorrelation function $g^2(t)$, a helium-neon laser (wavelength $\lambda=632.8$ nm), and a thermostat sample holder. Volume-weighted hydrodynamic diameters (D_H) of the flower micelles were obtained by CONTIN analysis. Changes in scattering intensity were measured at 90°. D_H reported in the paper is the average value from more than 10 measurements. Flower micelles in the dry state were also examined by using a Hitachi H-7500 transmission electron microscope (TEM) operating at 60 KV. Samples were prepared by casting a polymer solution at a chosen

temperature on a carbon-coated copper grid pre-heated to the same temperature; followed by drying at the temperature before cooling to room temperature for the observation. Fluorescence emission spectra of Nile Red loaded in flower micelles were recorded on a Varian Cary Eclipse spectrometer. Encapsulation of the hydrophobic dye by the micelles was obtained by adding 25 μL of a THF solution of Nile Red (0.5 mg/mL) into 4mL of a polymer solution at room temperature, which was followed by more than 6 h of stirring to evaporate THF. Finally, size exclusion chromatograph (SEC) measurements were performed on a Waters system equipped with a refractive index detector (RI 410) and a photodiode array detector (PDA 996). THF was used as the eluent at an elution rate of 1 mL/min, while polystyrene (PS) standards were used for calibration.

3. ^1H NMR, UV-vis and Fluorescence Spectroscopic Results

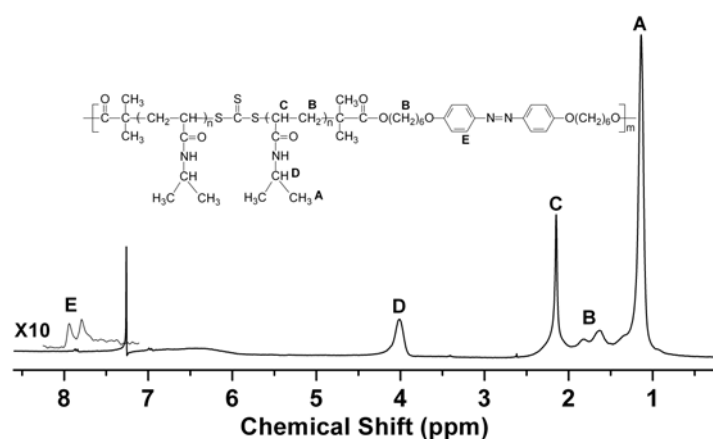


Figure S1 shows the ^1H NMR spectrum of P2 in CDCl_3 . The amount of PNIPAM with respect to azobenzene moieties could be determined by comparing the integrals of peak D at $\delta=3.98\text{-}4.20$ ppm and peak E at $\delta=7.80$ ppm. Combining with $M_n \sim 4600$ g/mol for the azobenzene-containing CTA (from SEC), the NMR analysis yielded $M_n \sim 44300$ g/mol for P2. Similar analysis gave rise to $M_n \sim 31600$ g/mol for P1.

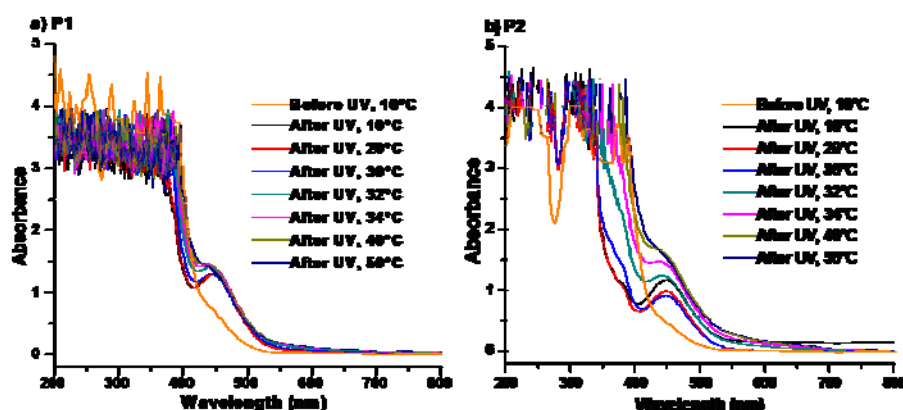


Figure S2 shows variable-temperature UV-vis spectra of the P1 and P2 solutions. In both cases, the absorption band of cis-azobenzene around 450 nm largely remained after the process of stepwise heating (2 $^\circ\text{C}$ interval), thermal equilibrium (5 min) and measurement.